CHEMISTRY
A EUROPEAN JOURNAL

DOI: 10.1002/chem.200601361

Hydrogen-Bonded Dendronized Polymers and Their Self-Assembly in Solution

Dang Xie,[a] Ming Jiang,*[a] Guangzhao Zhang,[b] and Daoyong Chen[a]

Abstract: Frechet-type benzyl ether dendrons of second and third generations with a carboxyl group (G2, G3) at the apex site could attach to poly(4-vinylpyridine) (PVP), forming hydrogen-bonded dendronized polymers (HB denpols) in their common solvent, chloroform. The HB denpols show unique self-assembly behavior, forming vesicles in the common solvent under ultrasonic treatment. The structure and morphology of the vesicles were characterized by dynamic light scattering (DLS), static light scattering (SLS), SEM, TEM, and AFM. The size of the vesicles decreases and the thickness of the vascular membrane increases as the molar ratio of G*x*/PVP increases. The hydrogen bonding, π–π aromatic stacking of the dendrons, and the considerable difference in architecture between the dendron G*x* and PVP are the main factors facilitating the assembly of the HB denpols in the common solvent.

Keywords: dendronized polymers · denpols · hydrogen bonds · self-assembly · vesicles

Introduction

Dendronized polymers (denpols) are newly emerged architectural macromolecules that consist of a linear main chain and bulky dendron grafts.[1] Another type of multicomponent polymer consisting of dendrons is the dendron-linear block copolymers, in which the dendron(s) attach to one of two ends of the linear polymer. For simplicity, we can call the former graft "denpols" and the latter "block denpols". In either case, the dendrons are connected to the linear polymer by covalent bonds. Because there is a significant architectural asymmetry between the dendrons and the linear polymer chain, such denpols are expected to have characteristic self-assembly behavior both in bulk and in solution. During the last decade, self-assembly of the denpols has been extensively studied.[2] The micelles built by block denpols are more stable than those of the conventional, linear, block copolymers[3] and they have a broad variety of morphologies, including some unconventional shapes.[4] Block denpols exhibit strong phase separation even when the enthalpic contributions to the separation are minor. This means that the molecular architecture of the denpols can play a key role in constructing a given morphology.[5] Percec et al. systematically studied the self-assembly of graft denpols in bulk.[6] However, as far as we know, little attention has been paid to the self-assembly of the graft denpols in solution. This is probably because the graft denpols with higher-generation dendrons form large molecular objects with a near-cylindrical shapes[7] and the main chain is buried into the dendrons. Thus, their self-assembly in solution would be hampered.

Here, we study the assembly behavior of *hydrogen-bonded* dendronized polymers (HB denpols) consisting of a linear polymer main chain with dendrons attached through hydrogen bonds. The general idea underlying this study stems from our long-term investigation of the "block copolymer-free strategy" in macromolecular assembly.[8] We reported that "graft copolymers" with a linear main chain and oligomers attached through hydrogen bonds can form micelles in *selective solvents*. As only hydrogen bonds connect the shell and core of the micelles, they are called noncovalently connected micelles (NCCM).[9] In the present study, the linear oligomer is replaced by dendrons so that architectural factors are introduced into the polymeric building blocks. This new type of denpol, comprising dendrons connected to a linear polymer by hydrogen bonds, displays a

[a] D. Xie, Prof. M. Jiang, D. Chen
Department of Macromolecular Science and
The Key Laboratory of Molecular Engineering of Polymers
Fudan University, Shanghai 200433 (P.R. China)
Fax: (+86) 21-6564-0293
E-mail: mjiang@fudan.edu.cn

[b] Prof. G. Zhang
Hefei National Laboratory for Physical Sciences at Microscale
Department of Chemical Physics
University of Science and Technology of China, Hefei (P.R. China)

Supporting information for this article is available on the WWW under http://www.chemeurj.org/ or from the author.

unique self-assembly characteristic of nanosized hollow objects formed in their *common solvent.* This would provide insight into the influence of architecture on self-assembly.[10]

Results and Discussion

Synthesis of Frechet-type benzyl ether dendrons with carboxylic acid groups at the apex (G*x*): Details of synthesis of the dendrons G*x* are described in the Experimental Section. As an example, the synthetic steps of G3 are shown in Scheme 1. The procedure is similar to that reported by Frechet et al,[25] however, we used 3,5-dihydroxyl benzoic acid **1** instead of 3,5-dihydroxyl benzyl alcohol as the starting material. In our procedure, after protecting the acid group, the coupling step gives the product in high yields after simple purification by column chromatography. Furthermore, our target G*x* with a carboxyl group at the apex can be easily obtained by hydrolysis of the methyl benzoate group of the products of each coupling reaction. The ^{1}H NMR spectrum of G3 is shown in Figure 1. In addition, poly(4-vinylpyridine) (PVP) with a narrow molecular-weight distribution was prepared by reversible addition-fragmentation chain-transfer polymerization (RAFT)[23] and its gel-penetration chromatography (GPC) curve is shown in Figure 2.

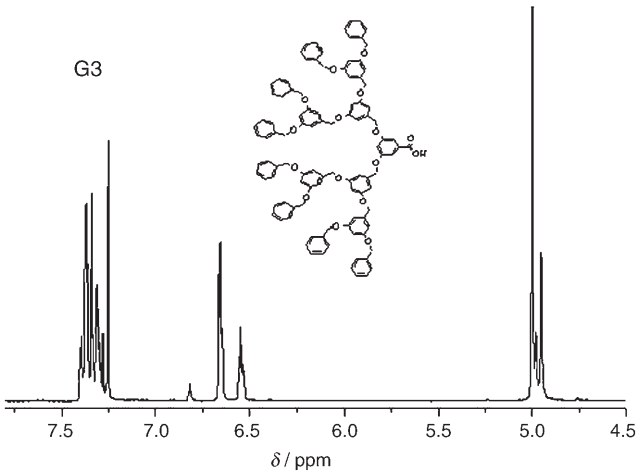

Figure 1. ^{1}H NMR spectrum ($CDCl_3$) of G3.

Self-assembly of HB denpols: Mixing a chloroform solution of G*x* with that of PVP produced a transparent solution, in which "graftlike" dendronized polymers were expected to form through hydrogen bonds between the carboxyl group at the dendron apex and the pyridine group of PVP (Figure 3). The formation of the hydrogen bonds is supported by ^{13}C NMR and IR spectroscopy measurements. For example, the signal of the carboxyl carbon of G2 solution in chloroform shifts from 171 to 169 ppm upon addition of PVP solution (1:1, w/w), which reflects that the self-association of the carboxyl is disrupted and an intermolecular hydrogen bond forms between the carboxyl hydroxyl group and the pyridyl group (Figure 4). In addition, in the spectrum of the blend solution, the peak at 170 ppm totally disappears, which denotes that these dendrons have completely attached to the PVP chains. This result is similar to that observed previously in linear hydrogen-bonded "graft" copolymers.[9b,11] The FTIR spectra (Figure 5) of the blend solutions also qualitatively reflect the hydrogen-bonding interaction between pyridyl and carboxyl, as the stretching bond of carboxyl shifts from 1691.3 to 1697.1 cm^{-1} upon mixing of the two solutions.

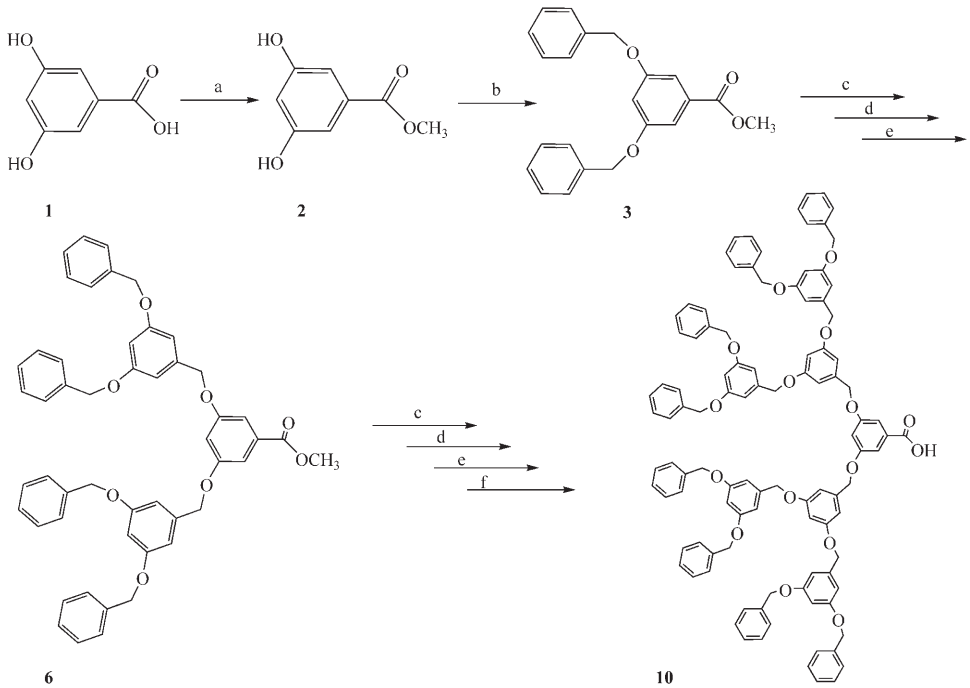

Scheme 1. Synthesis of G3. a) TsOH, MeOH, reflux 24 h; b) BnCl, K_2CO_3, KI, [18]C-6, acetone, reflux 12 h; c) $LiAlH_4$, THF, reflux; d) CBr_4, PPh_3, THF, RT; e) methyl 3,5-dihydroxy-benzoate, K_2CO_3, KI, [18]C-6, acetone, reflux; f) KOH, MeOH/H_2O, reflux.

Although mixing G*x* ($x=0$, 1, 2, 3, and 4) and PVP solutions in chloroform can lead initially to clear solutions, for G2/PVP and G3/PVP solutions, a tinge of blue opalescence appeared and gradually darkened after ultrasonic treatment for 10 min or longer. This unexpected phenomenon indicates the formation of intermolecular aggregates of G2 or G3 with PVP in their *common solvent*. Dynamic light scattering (DLS) and

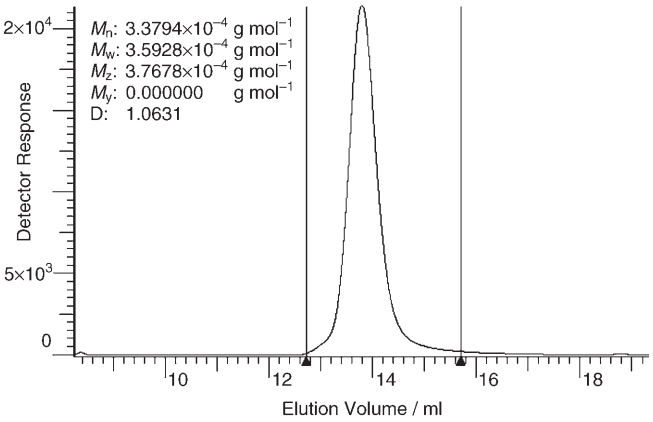

Figure 2. GPC trace for PVP synthesized by RAFT (DMF eluent).

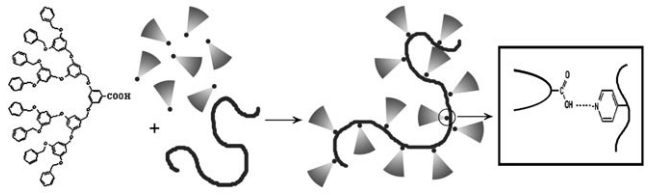

Figure 3. Chemical structure of dendron G3 and a schematic illustration of the formation of the H-bonded dendronized polymer.

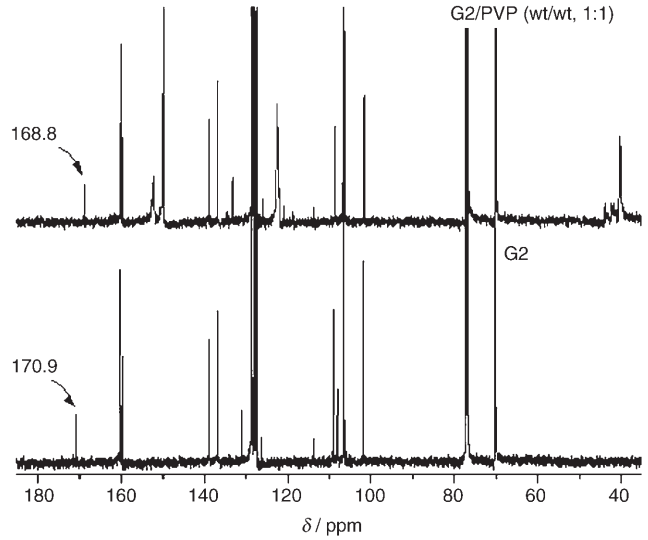

Figure 4. ^{13}C NMR results of G2 and the mixture of G2/PVP 47 in $CDCl_3$.

static light scattering (SLS) were used to characterize the aggregate solutions of G3/PVP over a broad composition range, that is, weight ratios of G3 and PVP, W_{G3}/W_{PVP}, from 0.16 to 4.2 and corresponding molar ratios of G3 and PVP, M_{G3}/M_{PVP}, from 3.6 to 90. (In this paper, we use molar ratio otherwise specified. For example, G3/PVP 10 denotes the sample with a M_{G3}/M_{PVP} of 10/1.) The DLS results are shown in Figure 6. Over such a broad composition range, intermolecular self-assembly takes place, forming aggregates

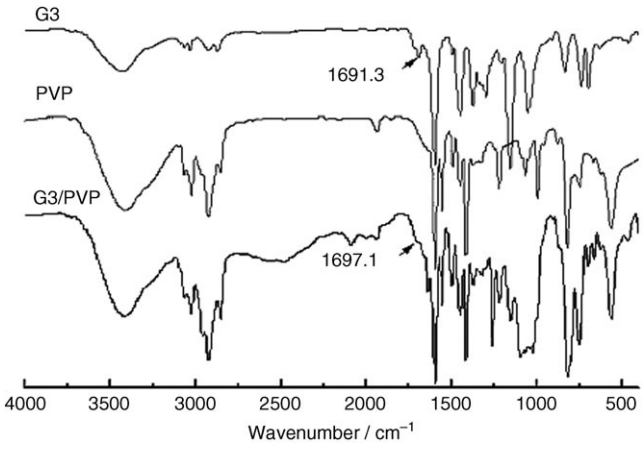

Figure 5. IR spectra of PVP, G3, and their blends G3/PVP 10.

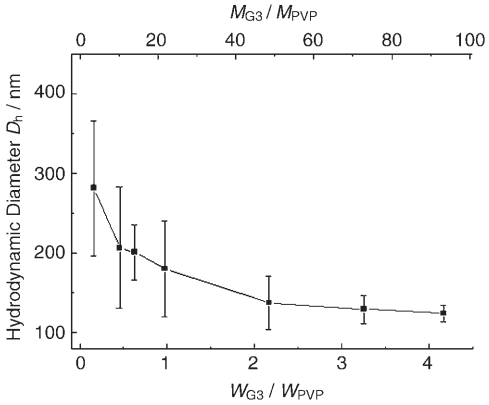

Figure 6. Hydrodynamic diameter versus the molar ratio (M_{G3}/M_{PVP}) and weight ratio (W_{G3}/W_{PVP}) of G3/PVP. The bar shows the size range measured for the samples with the same composition.

with average diameters from 100 to 400 nm. The results show a general trend of decreasing diameter as the relative amount of the attached dendrons to the main chain increases. We noticed that there is a substantial size fluctuation, particularly if the ratio M_{G3}/M_{PVP} is small. This reflects that the size of the aggregates is very sensitive to ultrasonic treatment, and the size reproducibility is usually poor from sample to sample. However, the aggregates show relatively narrow size distributions (polydispersity index (PDI) = 0.1, Figure 7). The SLS measurements show that the apparent "molecular weights" (M_W) of the aggregates are in the range of 1.06×10^7–2.2×10^8 g mol^{-1} (for an example, see Figure 8). By combining the results of DLS and SLS, we obtained the ratio of the average radius of gyration $\langle R_g\rangle$ to the average hydrodynamic radius $\langle R_h\rangle$ of the aggregates (Table 1). The $\langle R_g\rangle/\langle R_h\rangle$ values are around 1. This result implies that G3 and PVP possibly self-assemble to form a hollow structure.[12,13]

G2 and PVP show similar behavior, forming aggregates over a broad range of composition (data not shown). However, G0/PVP and G1/PVP, in which the intermolecular hydrogen bond formed easily, did not behave in this way, so

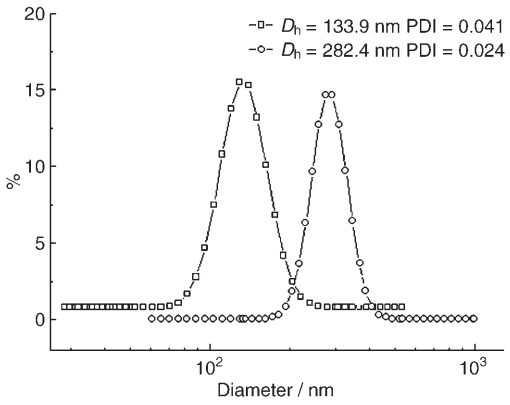

Figure 7. Typical D_h distribution curves: □: G3/PVP 23, ○: G3/PVP 10.

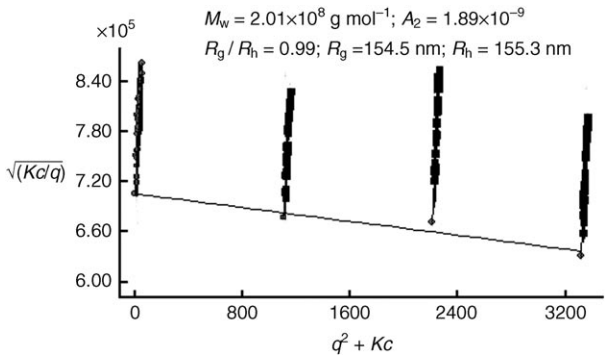

Figure 8. Berry plot of the aggregates of G3/PVP 10.

Table 1. $\langle R_g\rangle/\langle R_h\rangle$ data of G3/PVP at different molar ratios, determined by SLS.

M_{G3}/M_{PVP}	3.63	3.92	4.43	5.17	10.0	23.2
$\langle R_g\rangle/\langle R_h\rangle$	1.03	0.99	1.02	1.02	0.99	1.01

that the solutions remained clear over prolonged ultrasonic treatment. This implies that the π–π stacking force may play the key role in self-assembly,[14,20] as G2 and G3 possess larger cooperative stacking forces than the smaller dendrons of G0 and G1. However, the largest dendron G4, believed to have the strongest stacking force, did not show such a self-assembly ability with PVP. Here, we must consider the fact that the G4 molecule is so large that the carboxyl group at the apex would be buried by the peripheral benzyl ether groups,[15] thus, it could not contact the PVP chain. From this fact, we realized that the hydrogen bonding within the G*x*/PVP is vital to the self-assembly of micelles.

Self-assembly into large and thin-layer vesicles: We will now discuss the self-assembly of G3/PVP 10 in detail, in which each PVP chain has on average ten dendrons attached. G3/PVP 10 formed aggregates with a hydrodynamic diameter (D_h) of 282 nm (Figure 7) and $\langle R_g\rangle/\langle R_h\rangle = 0.99$ (Figure 8). Results of TEM studies show that the aggregates have a spherical shape (Figure 9a and Supporting Information Figure S1). The size and its narrow distribution are in generally agreement with the LS results. However, the particle images

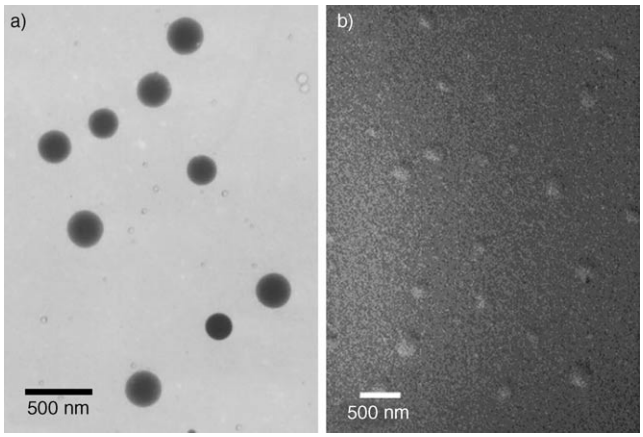

Figure 9. a) TEM and b) SEM images of the aggregates with $M_{G3}/M_{PVP} = 10$ without cross-linking.

in Figure 9a do not show any change in darkness from the center to the periphery, so that the aggregates look like solid spheres rather than hollow ones. Nevertheless, the SEM observations of the sample on mica (Figure 9b) show only blurry circular objects with poor contrast to the background. This image is very different from that expected for solid spheres with a diameter of around 300 nm.

A close examination of AFM results (Figure 10) clarifies this apparent discrepancy. Both the height and phase images show round outline shapes and diameters similar to those observed by TEM and SEM. The height analysis (Figure 10c) of these aggregates is of significant importance. The height of the aggregates was around 9 nm, one order of magnitude smaller than the average diameter determined by LS. Clearly, what we observe here are collapsed hollow spheres or vesicles, like two-layered cakes. These collapsed assemblies have an almost uniform thickness from the edge to the center, so that no contrast between the center and the periphery was observed in the TEM images. For the same reason, SEM can reveal only blurry circles. In fact, a similar TEM image for collapsed vesicles made of block codendrons was reported by Wang et al.[17]

It is known that soft vesicles can be reinforced by cross-linking the membrane. Cross-linking of PVP shells was carried out by reaction with 1,4-diiodobutane. The SEM images of these cross-linked aggregates (Figure 11a and Supporting Information Figure S2) display the integrate spheres with strong contrast to the background as a result of structure locking of the vesicles. The relative darkness of the central part of the spheres indicates that the membrane may partially sink during solvent evaporation. On the other hand, the TEM image (Figure 11b) of these cross-linked aggregates clearly shows typical vesicular morphology, although the membrane is much thicker (around 20 nm, Figure 11b inset)

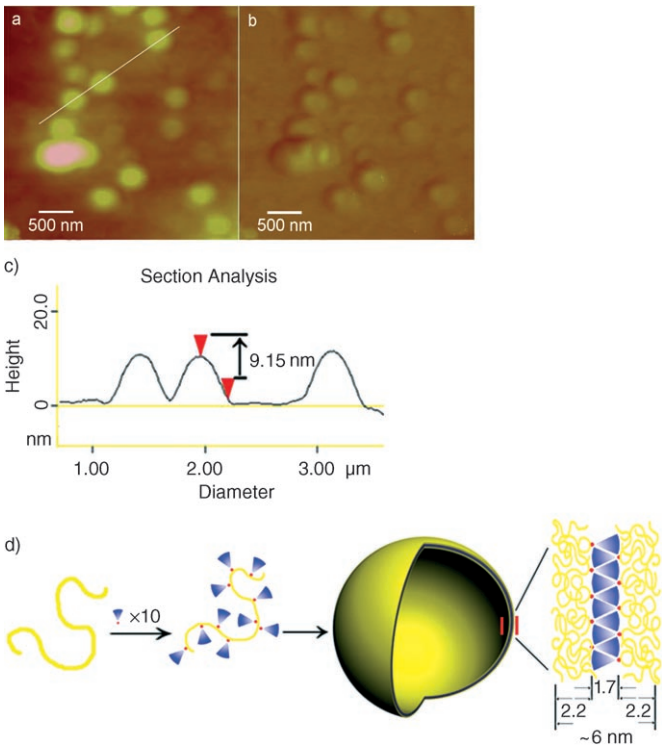

Figure 10. a) Height and b) phase AFM images of the aggregates of G3/PVP 10. c) AFM scan line for the particle-height analysis. d) Schematic illustration for the formation of the soft vesicle showing calculation of the membrane thickness.

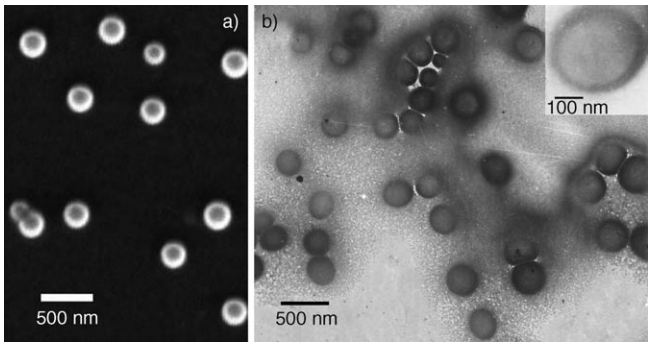

Figure 11. a) SEM and b) TEM images of the aggregates of the G3/PVP 10 sample after being cross-linked.

than that measured from AFM before cross-linking (Figure 10c). Clearly, incorporation of a comparative amount of cross-linker 1,4-diiodobutane extended the membrane.

In tapping mode AFM with soft materials, the measured height does not exactly correspond to the true height[16] and is usually less, due to the deformation of the soft surface by the AFM tip. As this may cause a 3-nm margin,[17] in the present case, the actual height of the two overlapping layers could be around 12 nm. This means that the thickness of the vesicle membrane is about 6 nm. We can now do a rough calculation of the membrane thickness for G3/PVP 10: On average, ten dendrons are attached to a PVP chain with a M_w of 3.6×10^4 g mol^{-1}. If we assume that the bulk density of PVP is 1, then the average diameter of a segment of PVP chain assigned to a dendron is close to 2.2 nm. Meanwhile, the geometric diameter of the G3 dendron is measured to be 1.7 nm.[18] Thus, the vesicle thickness is about 6 nm (Figure 10d), which matches the value measured from AFM, if we assume the membrane has a PVP/dendron/PVP sandwich structure. In other words, within the approximations involved above, the sandwich model satisfies the experimental observations.

Our sandwich model of the assembly membrane found support from simple solubility estimations. If toluene, a poor solvent for PVP, was added into the solution of G3/PVP vesicles in chloroform, precipitation took place. However, if methanol, a poor solvent for G3, was added, the system remained stable without precipitation. This test simply shows that PVP is located on the membrane surface while G3 is in the middle.

Self-assembly into small and thick-layer vesicles: We now discuss the self-assembly of dendron G3 and PVP with a much higher G3 content, that is, G3/PVP 23. The TEM (Figure 12a) and SEM (Figure 12b) images of the resulting aggregates are distinctly different from that of G3/PVP 10. The TEM result presents a typical characteristic of vesicles, that is, a clear contrast between the center and the periphery. From the TEM image, we can estimate approximately the thickness of the membrane (Figure 12a inset) to be around 30–40 nm. The SEM shows that the vesicles without cross-linking could basically sustain the spherical shape after evaporation of solvent. Thus, relative to the vesicles of G3/PVP 10, the vesicles of G3/PVP 23 are smaller and their membranes are thicker. Thus, they have better strength as they are able to keep their integrate during the sample-

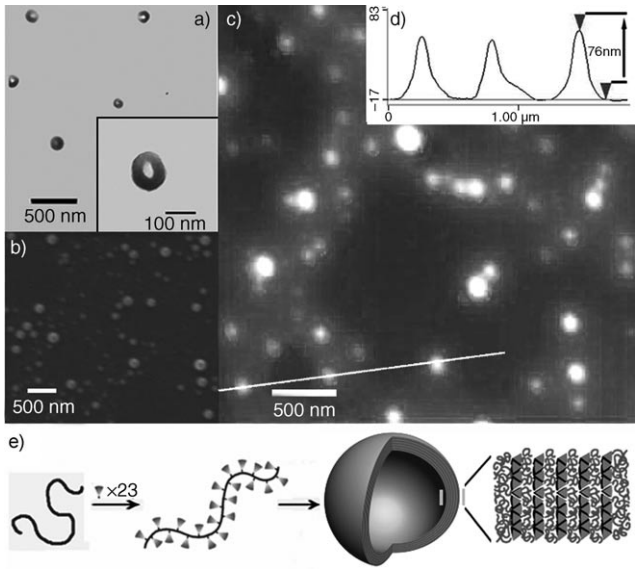

Figure 12. Vesicle (G3/PVP 23) image of a) TEM, b) SEM on mica, c) AFM on mica, d) AFM scan line, and e) a schematic illustration for the formation of the vesicle.

drying process. In addition, the light scattering results, that is, $\langle R_g\rangle/\langle R_h\rangle \approx 1.01$ (Table 1) and $D_h \approx 134$ nm (Figure 7) are generally in agreement with the TEM and SEM observations.

This opinion was supported by our AFM studies that showed spherical particles with a height of around 76 nm (Figure 12c,d). However, the vesicles are not completely collapsed here, so this value may include a contribution from the central cavity. As the estimated thickness of a PVP/dendron/PVP sandwich is around only 6 nm, we intend to think that the membrane of G3/PVP 23 contains several alternative G3 and PVP layers (Figure 12e).

Mechanism of vesicle formation: To monitor the process of the vesicle formation by DSL, we prepared a G3/PVP 45 solution with a short (2 min) ultrasonic treatment to initiate micellization. The solution was then centrifuged to ensure its dust-free treatment. The first DLS measurement (Figure 13) was performed 30 min after solution mixing.

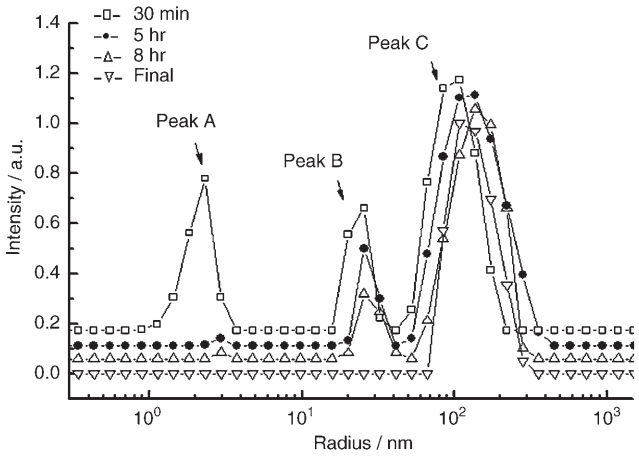

Figure 13. DLS trace of the HB-denpol solutions (G3/PVP 45) measured after different times.

There are three clear peaks, denoted A, B, and C. Peak A locates within the radius range of 1–4 nm and can be assigned to the individual G3 and PVP molecules. Peak C at around 100 nm probably corresponds to the aggregate particles. Peak B, between peaks A and C, covering a radius range of 20–40 nm can, in our opinion, be assigned to the soluble G3/PVP complex, that is, the hydrogen-bonded dendronized polymer. The results show that in solution, the individual G3 and PVP, the HB denpol, and the aggregate particles coexist. By comparing the curves measured at 0.5, 5, and 8 h, we can clearly see that the size of the aggregate particles gradually increases as peaks A and B decrease. After 8 h, the peak of individual molecules decreases dramatically, but can still be detected. Prolonging the standing time of the solution further caused a slight change in the intensity distribution only (data not shown). Finally, the solution was treated ultrasonically again for 3 min, after which both peaks A and B disappeared completely, indicating that G3 and PVP completely assembled into the particles without remnants of the individual molecules ("final" curve, Figure 13). This kinetic study qualitatively proves that in the mixed solutions of G3 and PVP, the soluble HB-denpol-polymer is an intermediate in the assembly, and ultrasonic treatment greatly promotes the process of self-assembly.

Although we are unable to present the assembly mechanism in detail here, we think the following facts play important roles in the assembly. Firstly, the π–π aromatic stacking of the dendrons may serve as the driving force. That such aromatic stacking of dendrons leads to self-assembly of block and graft denpols in their selective solvents is commonly accepted.[19] These π–π interactions are crucial for the stabilization of the self-assembly and for further formation the vesicles.[20] However, in our case, assembly takes place in the *common solvent*. Because in the present case, hydrogen bonds instead of chemical bonds connect the dendrons and PVP chains, it is quite possible that the dendrons could adjust their bonding sites along the PVP chains so as to favor the π–π stacking even in the common solvent. Secondly, because ultrasonic treatment was necessary for the formation of the vesicles, this may promote the dendrons to move to favorable positions for further aggregation. In addition, it was reported that the poly(benzyl ether) dendrons assume a constrictive conformation[18] in chloroform, which of course favors the aggregation of the dendritic molecules. Another important fact that shouldn't be overlooked is the architectural effect. In this combination of sector-type dendrons and linear PVP chains, the architectural asymmetry is prominent and provides an additional entropic effect on self-assembly due to the linear chain being unable to penetrate the sectors.[18,21] By forming the alternative layer-by-layer (PVP/dendron/PVP) structure of the vesicles, G3 and PVP could maximally reduce the interfacial free energy.

Conclusion

As illustrated schematically in Figure 10d and Figure 12e, the dendrons (G2, G3) with a carboxyl at the apex could form hydrogen-bonded dendronized polymers (denpols) with poly(4-vinylpyridine) (PVP) in their common solvent, chloroform. These denpols were able to self-assemble into stable nanosized aggregates, initiated by ultrasonic treatment in the solvent over a broad range of G*x*/PVP molar ratios. The denpol of G3/PVP 10 formed larger, soft vesicles with thin membranes with a PVP/G3/PVP three-layer structure (Figure 10d). As the G3/PVP ratio increased to around 23, the assemblies retained their vesicular structure, but had much smaller sizes and thicker membranes, with alternate G3/PVP layers (Figure 12e). Such self-assembly behavior in common solvent differs from that of the conventional block denpols that occurs in selective solvent only.

Experimental Section

Materials: Unless otherwise noted, materials were obtained from commercial suppliers and were used without further purification. 3,5-Dihy-

droxybenzoic acid (97%, Acros), [18]crown-6 ([18]C-6; 99%, Acros), lithium tetrahydroaluminate ($LiAlH_4$; typically 97%, Alfa), carbon tetrabromide (CBr_4; 99%, Aldrich), potassium iodide (KI; Shanghai Chemicals), *p*-toluenesulfonic acid (TsOH; 99%, Shanghai Chemicals), anhydrous potassium carbonate (K_2CO_3; AR, Shanghai Chemicals), benzyl chloride (BnCl; CP, Shanghai Chemicals), triphenyl phosphine (PPh_3; CP, Shanghai Chemicals), 1,4-diiodobutane (99%, Acros) were used as received. 2,2′-Azobis(isobutyronitrile) (AIBN; CP, Shanghai Chemicals) was purified by recrystallizing from methanol twice. Cumyl dithiobenzoate (CDB) was synthesized as described elsewhere.[22] 4-Vinylpyridine was distilled from CaH_2 under an atmosphere of nitrogen. Tetrahydrofuran (THF) was distilled from sodium/benzophenone under an atmosphere of nitrogen immediately before use. Acetone was dried with anhydrous potassium carbonate. Other reagents were used without further purification.

Techniques: ^{1}H NMR (400 MHz or 500 MHz) and ^{13}C NMR (125 MHz) spectra were recorded by using a Varian Gemini 200 or a Bruker DRX-500 spectrometer, respectively. $CDCl_3$ was used as solvent and TMS as internal standard, otherwise specified. The purity of products was determined by a combination of thin-layer chromatography (TLC) on silica-gel-coated aluminium plates (Kodak) with fluorescent indicator, and ^{1}H NMR spectrometry. Matrix-assisted laser desorption ionization time-of-flight (MALDI-TOF) mass spectra were recorded by using an Applied Biosystems Voyager-DE STR, using *trans* 3-indoleacrylic acid as the matrix, observing reflector-positive ions. Malvern Autosizer 4700 and ALV/SP-125 laser light scattering (LLS) spectrometers were used. DLS measurements were performed at a fixed scattering angle (θ) of 90°. Static LLS studies were conducted at a low scattering angle ranging from 15 to 30°. The $\langle D_h \rangle$ and polydispersity index (PDI, i.e., $(\langle \mu_2 \rangle / I^2)$ were obtained by a cumulant analysis. The respective *dn*/*dc* data of G3 and PVP were determined to be 0.180 and 0.159, respectively, in chloroform solution by using an Optilab DSP differential refractometer. TEM observations were performed by using a Philips CM 120 electron microscope at an acceleration voltage of 80 KV. For all TEM observations, the solutions of micelles were dropped onto the carbon-coated copper grids in an ambience of chloroform. SEM was conducted by using a Tescan 5136 MM scanning electron microscope. The AFM images were acquired in tapping mode by using a Nanoscope IV from Digital Instruments equipped with a silicon cantilever with 125 ímand E-type vertical engage piezoelectric scanner. For SEM and AFM observations, the samples were prepared by drying the solution in an ambience of chloroform on freshly cleaved mica at RT. PVP (PDI = 1.06, $M_w = 3.6 \times 10^4$ g mol^{-1}) was synthesized by reversible addition-fragmentation chain-transfer polymerization (RAFT)[23] and characterized by gel-penetration chromatography (GPC, Agilent 1100) (DMF eluent, 1.0 mL min^{-1}, 70 °C, Polymer Labs PL gel 5 μm mixed C column (molecular weight range 200–2000 K). Detection was by UV absorbance at 254 nm.

Micellization: Chloroform stock solutions (1 mg mL^{-1}) of G3 and PVP were mixed under ultrasonic treatment in different molar ratios and the mixed solutions then were treated ultrasonically for 20 min.

Vesicle cross-linking: Here, 1,4-diiodobutane was selected to cross-link the vesicles as previously reported.[24] Typically, 10 mol% of 1,4-diiodobutane, based on the repeating units of PVP and then the mixture, was kept stirred at RT for 24 h.

3,5-Dihydroxyl methyl benzoate (2): 3,5-Dihydroxyl benzoic acid (15 g, 0.1 mol), *p*-toluenesulfonic acid (3 g, 0.016 mol), and methanol (100 mL) were heated at reflux under N_2 for 24 h before methanol was removed in vacuo. The product was dissolved in ether, then washed with water and saturated $NaHCO_3$ solution. The organic layer was dried over $MgSO_4$, filtered, and concentrated in vacuo. Recrystallization from a mixture of CH_2L_2 and methanol and gave a white powder in 96% yield. ^{1}H NMR (500 MHz, $CDCl_3$, 25 °C, TMS): $\delta = 3.79$ (s, 3H; OCH_3), 6.44 (s, 1H; PhH), 6.81 (d, 2H; PhH), 9.61 ppm (s, 2H; OH).

Methyl 3,5-bis(benzyloxy) benzoate (G1−COOCH$_3$) (3): Compound **2** (11.18 g, 66.5 mmol), KI (5 g, 30.1 mmol), K_2CO_3 (20 g, 145 mmol), and [18]C-6 (200 mg, 0.76 mmol) were placed in dry acetone and were degassed with N_2 before addition of benzyl chloride (17 mL, 147.8 mmol). The mixture was heated at reflux under N_2 for 12 h and was monitored for completion by conducting TLC (petroleum ether/ethyl acetate 4:1). Acetone was removed in vacuo, the remaining solid was taken up in ethyl acetate (EA) (3×50 mL) and then washed with water (3×50 mL). The aqueous layer was extracted with EA (50 mL), and the combined organic products were washed with brine (50 mL), dried over $MgSO_4$, filtered, and concentrated in vacuo. Recrystallization from CH_2Cl_2/MeOH gave a white powder in 80% yield. ^{1}H NMR (500 MHz, $CDCl_3$, 25 °C, TMS): $\delta = 3.90$ (s, 3H; OCH_3), 5.07 (s, 4H; $PhCH_2O$), 6.80 (t, 1H; *p*-ArH to CO_2CH_3), 7.29–7.33 (d, 2H; *o*-ArH to CO_2CH_3), 7.33–7.43 ppm (m, 10H; PhH).

3,5-Bis(benzyloxy) benzyl alcohol (G1−OH) (4): Compound **3** (100 g, 312 mmol) in dry THF (350 mL) was added slowly over 1.5 h to a slurry of $LiAlH_4$ (2.57 g, 67 mmol) at 0 °C in dry THF (400 mL). Upon addition, the mixture was stirred at RT for 5 h, after which TLC (petroleum ether/ethyl acetate 1:1) confirmed completion. The reaction was cooled to 0 °C and quenched by successive additions of H_2O (13 mL) until H_2 evolution ceased. 1 N HCl was used to adjust the pH of the mixture to 7. The reaction mixture was then filtered and the lithium salts were rinsed generously with CH_2Cl_2. The filtrate was dried over $MgSO_4$ and was concentrated to give the crude product. The crude product was purified by flash column chromatography using silica gel/CH_2Cl_2 to give a white powder in 98% yield. ^{1}H NMR (500 MHz, $CDCl_3$, 25 °C, TMS): $\delta = 4.62$ (d, 2H; CH_2OH), 5.04 (s, 4H; $PhCH_2O$), 6.55 (s, 1H; *p*-ArH to CO_2CH_3), 6.62 (d, 2H; *o*-ArH to CO_2CH_3), 7.25–7.42 ppm (m, 10H; PhH).

3,5-Bis(benzyloxy) benzyl bromide (G1−Br) (5): Carbon tetrabromide (10.26 g, 31 mmol) was added to a stirred solution of compound **4** (8 g, 25 mmol) in dry THF (20 mL) under N_2. After stirring for 10 min, triphenylphosphine (8.29 g, 31 mmol) was added and the resulting reaction mixture was stirred for 1 h at RT, after which TLC (petroleum ether/ethyl acetate 3:1) confirmed completion. The reaction mixture was portioned between water (20 mL) and CH_2Cl_2 (20 mL). The organic layer was washed with water ((3×20 mL) and brine (20 mL), and the combined aqueous solutions were extracted twice with CH_2Cl_2. The combined CH_2Cl_2 solutions were dried over $MgSO_4$, filtered through Celite, and concentrated in vacuo to give the crude product. The crude product was purified by flash column chromatography using silica gel (petroleum ether/ethyl acetate 4:1) to give a white powder in 88% yield. ^{1}H NMR (500 MHz, $CDCl_3$, 25 °C, TMS): $\delta = 4.41$ (s, 2H; CH_2Br), 5.03 (s, 4H; $PhCH_2O$), 6.55 (s, 1H; *p*-ArH to CO_2CH_3), 6.64 (s, 2H; ArH), 7.31–7.42 ppm (m, 10H; PhH).

G2−COOCH$_3$ (6): A suspension of 3,5-dihydroxyl methyl benzoate (1.75 g, 10 mmol), KI (3.5 g, 21 mmol), K_2CO_3 (8.76 g, 63 mmol), and [18]C-6 ether (120 mg, 0.45 mmol) in dry acetone (100 mL) was heated at reflux under N_2 for 0.5 h before neat G1−Br (**5**) (8.76 g, 22 mmol) was added. The mixture was heated at reflux for 10 h before acetone was removed in vacuo. The crude product was dissolved in 50 mL CH_2Cl_2 and 50 mL H_2O. The aqueous layer was extracted with CH_2Cl_2 (3×50 mL). The combined CH_2Cl_2 solutions were washed with brine (100 mL), dried over $MgSO_4$, filtered, and concentrated in vacuo. The product was precipitated from CH_2Cl_2/MeOH and was purified by flash column chromatography in 25% ethyl acetate/75% petroleum ether. The product, a white powder, was isolated in 85% yield. ^{1}H NMR (500 MHz, $CDCl_3$, 25 °C, TMS): $\delta = 3.90$ (s, 3H; OCH_3), 5.00 (s, 4H; $ArCH_2O$), 5.03 (s, 8H; $PhCH_2O$), 6.57 (s, 2H; ArH), 6.67 (s, 4H; ArH), 6.76 (s, 1H; *p*-ArH to CO_2CH_3), 7.27–7.30 (d, 2H; *o*-ArH to CO_2CH_3), 7.35–7.42 ppm (m, 20H; PhH).

G2−OH (7): The procedure was similar to that for G1−OH. The product, a white solid, precipitated from CH_2Cl_2/MeOH and was collected on a glass frit to give the desired product in 94% yield. ^{1}H NMR (500 MHz, $CDCl_3$, 25 °C, TMS): $\delta = 4.62$ (d, 2H; CH_2OH), 4.97 (s, 4H; $ArCH_2O$), 5.03 (s, 8H; $PhCH_2O$), 6.52 (t, 1H; *p*-ArH to CH_2OH), 6.57 (t, 2H; ArH), 6.60 (d, 2H; *o*-ArH to CH_2OH), 6.67 (d, 4H; ArH), 7.27–7.41 ppm (m, 20H; PhH).

G2−Br (8): The procedure was similar to that for G1−Br. The product, a white powder, was isolated in 83% yield upon column chromatography in 50% ethyl acetate/50% petroleum ether. ^{1}H NMR (500 MHz, $CDCl_3$, 25 °C, TMS): $\delta = 4.40$ (s, 2H; CH_2Br), 4.96 (s, 4H; $ArCH_2O$), 5.03 (s, 8H; $PhCH_2O$), 6.51 (t, 1H; *p*-ArH to CH_2OH), 6.57 (t, 2H; ArH), 6.61 (d,

2H; *o*-ArH to CH_2OH), 6.67 (d, 4H; ArH), 7.30–7.42 ppm (m, 20H; PhH).

G3−COOCH$_3$ (9): The procedure was similar to that for G2−$COOCH_3$. The product, a white powder, was isolated in 80% yield upon column chromatography in 80% CH_2Cl_2/20% petroleum ether. ^{1}H NMR (500 MHz, $CDCl_3$, 25°C, TMS): δ=3.86 (s, 3H; OCH_3), 4.96–5.00 (3 s, 28H; $ArCH_2O$ and $PhCH_2O$), 6.53 (s, 2H; ArH), 6.55 (s, 4H; ArH), 6.65 (d, 4H; ArH), 6.66 (d, 8H; ArH), 6.82 (s, 1H; *p*-ArH to CO_2CH_3), 7.27–7.40 ppm (m, 42H; PhH, ArH, *m*-ArH to CO_2CH_3).

G3−COOH (10) and G2−COOH (11): G3−$COOCH_3$ (2.13 g, 1.30 mmol) was dissolved in THF (60 mL). The mixture was refluxed for 2 h before aqueous KOH (0.24 g, 4.18 mmol in 3.8 mL water) and MeOH (26 mL) was added. The product was dissolved in CH_2Cl_2 (3×50 mL) before removal of THF and neutralization of the mixture with 1N HCl. The CH_2Cl_2 solutions were washed with water (2×100 mL) and then with brine (100 mL). Removal of solvent in vacuo gave a white solid, isolated in 92% yield upon column chromatography in CH_2Cl_2.

Data for G3: ^{1}H NMR (500 MHz, $CDCl_3$, 25°C, TMS): δ=4.95 (s, 8H; $ArCH_2O$), 4.98 (s, 4H; $ArCH_2O$), 5.00 (s, 16H; $PhCH_2O$), 6.53–6.55 (m, 6H; ArH), 6.64–6.66 (m, 12H; ArH), 6.82 (t, 1H; J=2.6 Hz, *p*-ArH to CO_2H), 7.28–7.40 ppm (m, 42H; PhH and ArH); ^{13}C NMR ($CDCl_3$): δ= 70.01, 70.10 ($PhCH_2O$ and $ArCH_2O$), 101.69, 101.83, 106.42 and 106.54 (ArH), 108.07 (*p*-ArC to CO_2H), 108.99 (*o*-ArC to CO_2H), 127.50 (*o*-PhC to CH_2O), 127.93 (*p*-PhC to CH_2O), 128.53 (*m*-PhC to CH_2O), 130.91 (ArC next to CO_2H), 136.82 (PhC next to CH_2O), 138.83 and 139.23 (ArC), 159.76 (*m*-ArC to CO_2H), 160.10 and 160.17 (ArC), 169.60 ppm (CO_2H); MALDI-TOF MS: *m*/*z* calcd for $C_{105}H_{90}O_{16}$ $[M+Na]^+$: 1630.6; found: 1631.2, 1632.2, 1633.2, 1634.2, 1635.2 multipeaks.

Data for G2: ^{1}H NMR ($CDCl_3$): δ=5.01 (s, 4H; $ArCH_2O$), 5.03 (s, 8H; $PhCH_2O$), 6.58 (t, 2H; ArH), 6.68 (d, 4H; ArH), 6.81 (d, 1H; *p*-ArH to CO_2H), 7.30–7.32 (d, 2H; *o*-ArH to CO_2H), 7.35–7.42 ppm (m, 20H; PhH); ^{13}C NMR ($CDCl_3$): δ=70.20 ($ArCH_2O$), 101.87, 106.50 (ArH), 108.16 (*p*-ArC to CO_2H), 109.05 (*o*-ArC to CO_2H), 127.51 (*o*-PhC to CH_2O), 127.99 (*p*-PhC to CH_2O), 128.57 (*m*-PhC to CH_2O), 131.09 (ArC next to CO_2H), 136.81 (PhC next to CH_2O), 138.82 (ArC), 159.79 (*m*-ArC to CO_2H), 160.25 (ArC), 170.86 ppm (CO_2H); MALDI-TOF MS: *m*/*z* calcd for $C_{49}H_{42}O_8$ 781.3: $[M+Na]^+$; found: 782.2, 783.2, 784.2 multipeaks.

Poly(4-vinylpyridine) (PVP):[23] The homopolymer of 4-vinylpyridine (4-VP) was synthesized under bulk conditions by RAFT employing azoisobutyronitrile (AIBN) as the initiator and cumyl dithiobenzoate (CDB) as the RAFT chain-transfer agent (CTA). Polymerization was conducted at 60°C under a nitrogen atmosphere in septa-sealed vials. The initiator/CTA molar ratio was kept constant at 1:4.75 with an initial monomer concentration of 9.27M (bulk monomer). The CTA/monomer ratios ($[CTA]_0/[M]_0$=1:374) were such that the theoretical M_n at 100% conversion for 4-VP was 39300 g mol^{-1}. By quenching the polymerizations after 24 h, we obtained PVP with polydispersity indices (M_w/M_n) of 1.06 and M_w of 36 K.

Acknowledgements

The National Natural Science Foundation of China (NNSFC, Project Nos. 50333010) is acknowledged for supporting this research.

[1] A. D. Schlüter, J. P. Rabe, *Angew. Chem.* **2000**, *112*, 860–881; *Angew. Chem. Int. Ed.* **2000**, *39*, 864–883. A. Zhang; L. Shu, Z. Bo, A. D. Schlüter, *Macromol. Chem. Phys.* **2003**, *204*, 328–339; H. Frauenrath, *Prog. Polym. Sci.* **2005**, *30*, 325–384; A. D. Schlüter, *Top. Curr. Chem.* **2005**, *245*, 151–191.

[2] E. R. Gillies, T. B. Jonsson, J. M. J. Frechet, *J. Am. Chem. Soc.* **2004**, *126*, 11936–11943; B. K. Cho, A. Jain, S. M. Gruner, U. Wiesner, *Science* **2004**, *305*, 1598–1601.

[3] G. R. Newkome, C. N. Moorefield, G. R. Baker, R. K. Behera, G. H. Escamillia, M. J. Saunders, *Angew. Chem.* **1992**, *104*, 901–903; *Angew. Chem. Int. Ed. Engl.* **1992**, *31*, 917–919.

[4] I. Gisto, J. M. J. Frechet, *Macromolecules* **1993**, *26*, 6536–6546.

[5] M. E Mackay, Y. Hong, M. Jeong, B. M. Tande, N. J. Wagner, S. Hong, S. P. Gido, R. Vestberg, C. J. Hawker, *Macromolecules* **2002**, *35*, 8391–8399.

[6] V. Percec, C. H. Ahn, G. Ungar, *Nature* **1998**, *391*, 161–164; G. Ungar, Y. Liu, X. B. Zeng, V. Percec, *Science* **2003**, *299*, 1208–1211; V. Percec, M. R. Imam, T. K. Bera, *Angew. Chem.* **2005**, *117*, 4817–4823; *Angew. Chem. Int. Ed.* **2005**, *44*, 4739–4745; V. Percec, C. M. Mitchell, *J. Am. Chem. Soc.* **2004**, *126*, 6078–6094.

[7] C. Böttcher, B. Schade, C. Ecker, J. P. Rabe, L. J. Shu, A. D. Schlüter, *Chem. Eur. J.* **2005**, *11*, 2923–2928; J. Das, M. Yoshida, J. M. J. Frechet, A. K. Chakraborty, *J. Phys. Chem. B* **2005**, *109*, 6535–6543; C. Ecker, N. Severin, L. J. Shu, A. D. Schlüter, J. P. Rabe, *Macromolecules* **2004**, *37*, 2484–2489; A. F. Zhang, L. J. Shu, Z. S. Bo, A. D. Schlüter, *Macromol. Chem. Phys.* **2003**, *204*, 328–339.

[8] D. Y. Chen, M. Jiang, *Acc. Chem. Res.* **2005**, *38*, 494–503.

[9] a) S. Y. Liu, G. Z. Zhang, M. Jiang, *Polymer* **1999**, *40*, 5449–5453; b) S. Y. Liu, Q. M. Pan, J. W. Xie, M. Jiang, *Polymer* **2000**, *41*, 6919–6929; c) M. Wang, G. Z. Zhang, D. Y. Chen, M. Jiang, S. Y. Liu, *Macromolecules* **2001**, *34*, 7172–7178; d) M. Wang, M. Jiang, F. L. Ning, D. Y. Chen, S. Y. Liu, *Macromolecules* **2002**, *35*, 5980–5989.

[10] H. W. Duan, D. Y. Chen, M. Jiang, W. J. Gan, S. J. Li, M. Wang, J. Gong, *J. Am. Chem. Soc.* **2001**, *123*, 12097–12098.

[11] H. S. Peng, D. Y. Chen, M. Jiang, *Langmuir* **2003**, *19*, 10989–10992.

[12] C. Wu, S. Q. Zhou, *Phys. Rev. Lett.* **1996**, *77*, 3053.

[13] Note: Although there is a large fluctuation in the DLS measurements of $\langle R_h \rangle$ for the samples prepared at the same conditions, $\langle R_g \rangle / \langle R_h \rangle$ values do not show a substantial error, as both $\langle R_g \rangle$ and $\langle R_h \rangle$ were always measured simultaneously for the same sample.

[14] Y. K. Kwon, S. Chvalun, A. I. Schneider, J. Blackwell, V. Percec, J. A. Heck, *Macromolecules* **1994**, *27*, 6129–6132; Y. Ji, Y. F. Luo, X. R. Jia, E. Q. Chen, Y. Huang, C. Ye, B. B. Wang, Q. F. Zhou, Y. Wei, *Angew. Chem.* **2005**, *117*, 6179–6183; *Angew. Chem. Int. Ed.* **2005**, *44*, 6025–6029; E. R. Zubarev, M. U. Pralle, E. D. Sone, S. I. Stupp, *J. Am. Chem. Soc.* **2001**, *123*, 4105–4106; Y. K. Kwon, S. N. Chvalun, J. Blackwell, V. Percec, J. A. Heck, *Macromolecules* **1995**, *28*, 1552–1558.

[15] B. Helms, J. L. Mynar, C. J. Hawker, J. M. J. Frechet, *J. Am. Chem. Soc.* **2004**, *126*, 15020–15021.

[16] H. G. Hansma, *J. Vac. Sci. Technol. B* **1996**, *14*, 1390–1394; J. Tamayo, R. Garacia, *Langmuir* **1996**, *12*, 4430–4435.

[17] M. Yang, W. Wang, F. Yuan, X. Zhang, *J. Am. Chem. Soc.* **2005**, *127*, 15107–15111.

[18] M. Jeong, M. E. Mackay, R. Vestberg, C. J. Hawker, *Macromolecules* **2001**, *34*, 4927–4936.

[19] E. R. Zubarev, M. U. Pralle, E. D. Sone, S. I. Stupp, *J. Am. Chem. Soc.* **2001**, *123*, 4105–4106; J. J. Apperloo, R. A. J. Janssen, P. R. L. Manlenfant, J. M. J. Frechet, *Macromolecules* **2000**, *33*, 7038–7043.

[20] C. F. L. Ken, M. M. Paula, N. M. Sergei, H. N. Brian, K. Sangcheol, P. Kaushik, H. F. Amar, R. T. Hsian, J. F. Stoddart, *J. Am. Chem. Soc.* **2006**, *128*, 10707–10715.

[21] M. E Mackay, Y. Hong, M. Jeong, B. M. Tande, N. J. Wagner, S. Hong, S. P. Gido, R. Vestberg, C. J. Hawker, *Macromolecules* **2002**, *35*, 8391–8399.

[22] G. Tabak, T. N. Pham, G. Levesque, R. Haraoubia, *J. Polym. Sci. Part A: Polym. Chem.* **1998**, *36*, 117–127.

[23] A. J. Convertine, R. S. Sumerlin, D. B. Thomas, *Macromolecules* **2003**, *36*, 4679–4681.

[24] K. B. Thurmond, T. Kowalewski, K. L. Wooley, *J. Am. Chem. Soc.* **1996**, *118*, 7239–7240; M. Wang, M. Jiang, F. L. Ning, D. Y. Chen, *Macromolecules* **2002**, *35*, 5980–5989.

[25] C. J. Hawker, J. M. J. Frechet, *J. Am. Chem. Soc.* **1990**, *112*, 7638–7647.

Received: September 21, 2006
Published online: January 5, 2007

